Light Tracking and Light Guiding Fiber Arrays by Adjusting the Location of Photoresponsive Azobenzene in Liquid Crystal Networks

Document license:
CC BY-NC

DOI:
[10.1002/adom.202000732](https://doi.org/10.1002/adom.202000732)

Document status and date:
Published: 18/09/2020

Document Version:
Publisher's PDF, also known as Version of Record (includes final page, issue and volume numbers)

Please check the document version of this publication:

• A submitted manuscript is the version of the article upon submission and before peer-review. There can be important differences between the submitted version and the official published version of record. People interested in the research are advised to contact the author for the final version of the publication, or visit the DOI to the publisher's website.
• The final author version and the galley proof are versions of the publication after peer review.
• The final published version features the final layout of the paper including the volume, issue and page numbers.

Link to publication

Download date: 16. Nov. 2023

FULL PAPER

ADVANCED
OPTICAL
MATERIALS
www.advopticalmat.d

Check for
updates

Light Tracking and Light Guiding Fiber Arrays by Adjusting the Location of Photoresponsive Azobenzene in Liquid Crystal Networks

Li Liu, Marc del Pozo, Fateme Mohseninejad, Michael G. Debije, Dirk J. Broer,* and Albert P. H. J. Schenning*

The integration of light tracking and light guiding within fiber arrays is an intriguing challenge. In this study, an advanced drop casting/drawing method is applied to fabricate a fiber array capable of not only performing sunflower-inspired light tracking, but also light guiding. The fiber arrays are constructed with various liquid crystal networks by adjusting the location of photoresponsive azobenzene moieties in the polymer network to understand the correlation between the extent of photoresponse and azobenzene location. Incorporating the azobenzene in the main chain oligomer renders these fibers with advanced photoresponse in both air and water. The fibers are able to track a light source and to guide the collected light, making these responsive actuator arrays potentially attractive for advanced photovoltaic and optical elements.

L. Liu, M. del Pozo, F. Mohseninejad, Dr. M. G. Debije, Prof. D. J. Broer, Prof. A. P. H. J. Schenning
Stimuli-Responsive Functional Materials and Devices
Department of Chemical Engineering
Eindhoven University of Technology
P.O. Box 513, Eindhoven, MB 5600, The Netherlands
E-mail: d.broer@tue.nl; a.p.h.j.schenning@tue.nl
L. Liu
School of Chemistry and Chemical Engineering
Jiangsu Province Hi-Tech Key Laboratory for Bio-medical Research
State Key Laboratory of Bioelectronics
Institute of Advanced Materials
Southeast University
Nanjing 211189, China
Prof. D. J. Broer, Prof. A. P. H. J. Schenning
Institute for Complex Molecular Systems
Eindhoven University of Technology
Den Dolech 2, Eindhoven, MB 5600, The Netherlands
Prof. D. J. Broer, Prof. A. P. H. J. Schenning
SCNU-TUE Joint Laboratory of Device Integrated
Responsive Materials (DIRM)
South China Normal University
Guangzhou Higher Education Mega Center
Guangzhou 510006, China

The ORCID identification number(s) for the author(s) of this article can be found under https://doi.org/10.1002/adom.202000732.

1. Introduction

Tether-free actuation is of importance for developing soft robotics, microfluidic devices, responsive surfaces, and advanced optical materials.[1–3] Among various external energy sources, photon energy provides a promising and versatile platform to construct untethered actuators featured with a high degree of flexibility, accuracy, and programmability.[4–6]

Heliotropism, the motion of flowers or leaves in response to the position of the sun to maximize energy harvesting, provides inspiration for researchers for the development of light responsive materials and optical light guiding elements.[7] Heliotropism-like actuators have been developed to achieve light tracking in artificial fiber arrays based on a feedback loop involving photothermal effects and the mechanical properties of the polymers employed.[8] A photoactive light guiding actuator has been constructed to drive photothermal deformations.[9] For photothermal actuation, a specific chromophore is often added to the system so that when illuminated with the proper wavelength, a mechanical response is generated.[10–14] Once the illumination stops, the actuator immediately returns to its initial state due to the reduction of the temperature. Thus, a constant energy supply is essential to preserve the desired transitional conformation. In pursuit of shape morphing with long-lived and energy-efficient features, developing alternative photoactive polymers driven by a photochemical effect is of great interest. Photochemical actuation mostly depends on forward and backward isomerization of an incorporated molecular photoswitch activated and de-activated by using different wavelengths.[15,16] The material that we chose for the responsive fibers are based on oligomeric liquid crystal monomers decorated with a low molecular weight co-polymerizing crosslinker. In the design of the responsive fibers, we have different options for the position of the photoswitching molecules, either as being an integral part of the oligomeric monomers or as separately added crosslinking molecule. It is the objective of this research to determine the optimum fiber composition and to deploy these fibers in a light directing device.

Liquid crystal (LC) polymer networks containing azobenzene molecules are attractive for fabricating photochemically driven

ADVANCED
SCIENCE NEWS

www.advancedsciencenews.com
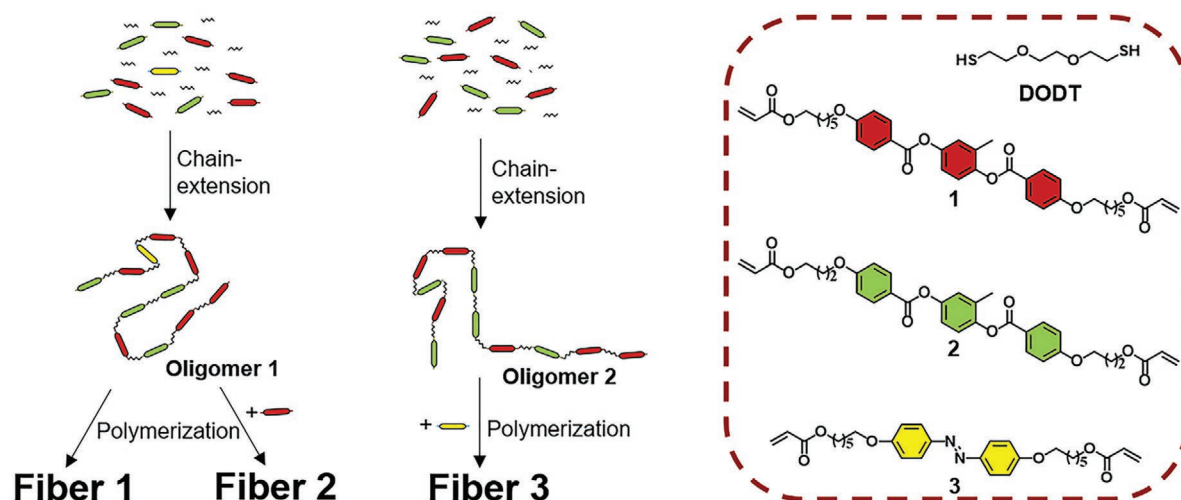
ADVANCED
OPTICAL
MATERIALS

www.advopticalmat.de

Figure 1. Synthetic routes and chemical composition for the fabrication of azobenzene-functionalized LC fibers.

soft actuators.[17–22] The rod-like shape of *trans*-azobenzene is compatible with mesogens, facilitating the LC network alignment.[23] Large and reversible geometrical changes between 9.0 and 5.5 Å accompany the *trans–cis* isomerization of azobenzenes.[24] The efficient and reversible molecular motion of network-embedded azobenzenes is amplified into macroscopic deformations in LC polymers. Recently, we reported on light-responsive fibers arrays prepared by a drop-casting and drawing method.[25] The polymer fibers were obtained in a two-step process in which a main chain liquid crystal oligomer was first synthesized by a Michael addition reaction, followed by mixing of the oligomer with the azobenzene and photoinitiator in the second step. The precursor mixture was melted and the fibers were drawn in the liquid crystalline state and photopolymerized. The fiber arrays showed efficient photoactuation mainly at elevated temperatures, hindering further applications of such novel materials under ambient conditions. Therefore, optimization of the material is desirable to fabricate light-responsive fiber arrays able to respond efficiently at room temperature.

In this work, we report a strategy for constructing advanced and multifunctional LC fiber arrays that are photoresponsive at room temperature in both air and when immersed in water. A systematic study was conducted to explore the impact of the location of azobenzene chromophores in the polymer network on the photomechanical response (**Figure 1**). Accordingly, azobenzene molecules were introduced into the LC polymer network during either the chain extension step (fibers 1 and 2) or the photo-crosslinking process (fiber 3).[24] Additionally, the fiber arrays were able to track and guide light, making them attractive for applications in light-responsive optical devices.

2. Results and Discussion

2.1. Fabrication and Characterization of Fibers

The initial goal was to design a main-chain LC oligomer with viscoelasticity suitable for drawing fibers from the melt state.[26–29]

To accomplish this, the thiol-acrylate Michael addition reaction between diacrylate mesogens and a flexible dithiol spacer was adopted.[30–33] Two types of oligomers, one with azobenzene (denoted as oligomer 1) and one without azobenzene (denoted as oligomer 2), were synthesized. A mixture of mesogenic diacrylate monomers of 1:1 stoichiometric ratio between **1** and **2** (Figure 1) was selected to optimize the mesogenic and viscoelastic properties of the oligomers.[34,35] Oligomerization between diacrylate LC monomers and dithiol chain extender was conducted at 38 °C overnight. A cross-linkable acrylate-terminated oligomer was synthesized by using a slight excess of acrylate (Table S1, Supporting Information). In the ^{1}H NMR spectra (Figures S1 and S2, Supporting Information), peaks of acrylic protons centered at 6.40–5.70 ppm confirmed the existence of acrylate end groups for post-polymerization. Gel permeation chromatography (GPC) revealed a weight average molecular weight (M_w) of the oligomers between 17 000 and 18 000 g mol^{-1} with a polydispersity index (M_w/M_n) ranging from 2.7 to 2.8 (Table S2, Supporting Information). In the GPC contour plot (Figure S3b, Supporting Information), the same retention time of the main absorption peak at ≈250 nm and the absorption peak of *trans*-azobenzene (Compound **3** in Figure 1) at ≈365 nm revealed that azobenzene molecules were incorporated in oligomer 1. Differential scanning calorimetry (DSC) revealed a clearing point (T_i) for both oligomers of around 72 °C (Figure S4, Supporting Information).

With these two acrylate-terminated oligomers in hand, fiber arrays on a glass substrate were fabricated via a drop casting/drawing method, which generates vertically standing fibers at specific positions with controlled dimensions and alignment on a substrate. Generally, the fiber length depends on the viscosity of the oligomer mixture and the distance between two glass slides used for drawing the fiber. If the mixture is not viscous enough and the spacing between two glass slides is too large, the fibers are susceptible to breakage during the drawing process or cannot maintain the vertical state after removal of the top glass slide. The oligomers, together with photoinitiator (fiber 1) and diacrylate monomers **1** and **3** (fibers 2 and 3, respectively), were first dissolved in dichloromethane to get a homogenous mixture.

**ADVANCED
SCIENCE NEWS**

www.advancedsciencenews.com

**ADVANCED
OPTICAL
MATERIALS**
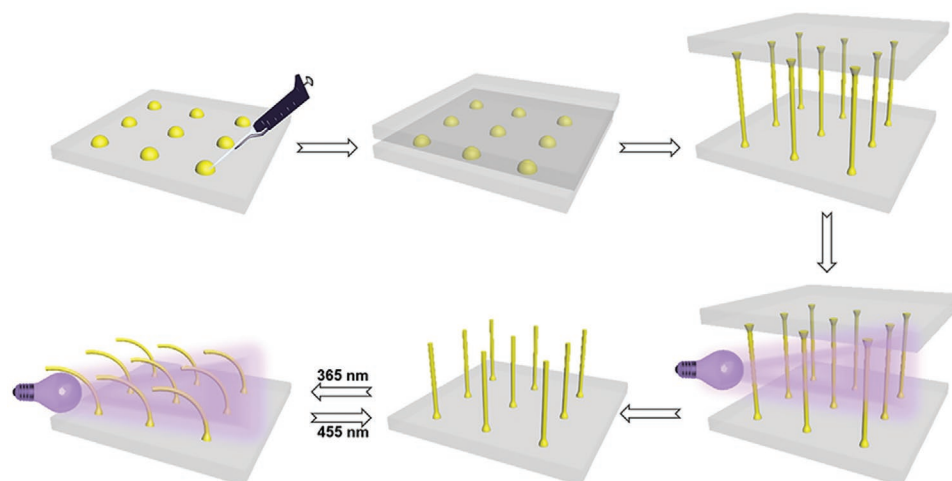
www.advopticalmat.de

Figure 2. Schematic illustration of the drop-casting procedure and reversible photoresponsive actuation of fibers.

Then, as shown in **Figure 2**, droplets were drop cast on a glass substrate and placed on a hotplate which was heated to evaporate the solvent. Subsequently, another glass plate was placed at a specific height over the substrate and just brought into contact with the droplets. Fibers were formed when the two glass plates were pulled apart, resulting in an alignment of the oligomers along the stretching direction.[25] After photo-polymerization in a nitrogen atmosphere for 1 h, fibers were cut away from one side of the glass plate to produce the standalone fiber arrays on glass.

The thermally activated deformation of the free-standing fibers in a silicon oil bath was recorded between crossed polarizers as a function of temperature. As seen in Figure S5 in the Supporting Information, all fibers contracted along the longitudinal axis (corresponding to the drawing direction) during heating, revealing the preferential oligomer alignment to be along the stretching direction.[36] The longitudinal shrinkage ratio (L/L_o), representing the negative anisotropic thermal expansion along the fiber axis, was plotted at elevated temperatures, where L represented the length of fiber at a specified temperature and L_o was the initial length of fiber at 25 °C. Fiber 1 reached its maximum shrinkage ratio (≈0.57) at ≈115 °C. In contrast, fibers 2 and 3, composed of oligomers mixed with diacrylate small molecules, reached their maximum contractions at higher temperature (135 °C). Such variation in the actuation temperature could be due to the presence of the crosslinking molecules that enhance the crosslink density in the network.

Wide-angle X-ray diffraction measurements were conducted to determine the order parameter (S) in the stretched fibers (Figure S6, Supporting Information).[37] The S values of 0.68 for fiber 1 and 0.69 for fiber 3 imply that mesogens are well aligned along the stretching direction. The similar values support that the location of the azobenzene within the fibers plays a decisive role in the photoactuation process (*vide infra*).

2.2. Photoactuation of Fibers

The photomechanical motions of the fiber arrays were initially examined in a dry environment under the illumination of

UV (365 nm, 75 mW cm⁻²) or visible (455 nm, 30 mW cm⁻²) light, corresponding to the characteristic absorption peaks of *trans-* and *cis-*azobenzene, respectively. Upon UV light irradiation, all fibers underwent a rapid bending behavior toward the light source. Such bending can be ascribed to the generated asymmetric gradient in concentration of *cis-*azobenzene chromophores, which results in reduced mesogenic order in the surface-exposed region, leading to contraction. Fibers recovered to their initial unbent states after illumination with visible light, which promotes *cis-*to-*trans* back isomerization. When the azobenzene moieties were used as the low molecular weight crosslinkers and copolymerized with the oligomeric monomer, the maximum light-induced bending angle is ≈25° in fiber 3. Under similar illumination conditions, fibers 1 and 2 containing the azobenzene chromophores in the main chain oligomer exhibited larger bending angles of 59° and 48°, respectively. Such amplified photo-deformable behaviors in fibers 1 and 2 are likely due to the efficient isomer-generated network stresses when both ends of azobenzene are connected to the main chain oligomer. It is speculated that the molecular freedom of the azobenzene moieties as part of the oligomeric main chain gives larger conformational changes than when they are embedded in the more restricted locations of the more densely crosslinked areas. This shows the importance of azobenzene location in the LC fibers. The time of maximum bending angle was 25 s for fiber 1 and 35 s for fibers 2 and 3, revealing that fiber 1 outperforms the other two fibers. Such distinct actuation of fiber 1 might benefit from the reduction of the network crosslink density. The times to attain maximum bending angle of fibers 2 and 3 were similar, which can be explained by the similar crosslink density in two fiber networks containing both oligomers and diacrylate small molecules. The photomechanical response of the fibers was tested over ten cycles with no obvious attenuation of the photoactuation. Fibers took a longer time to recover to their initial states than attaining their maximum bending deformation, which might be due to the relatively low light intensity (30 mW cm⁻²) of visible light used and the low light absorption of the *cis-*azobenzene at 455 nm.
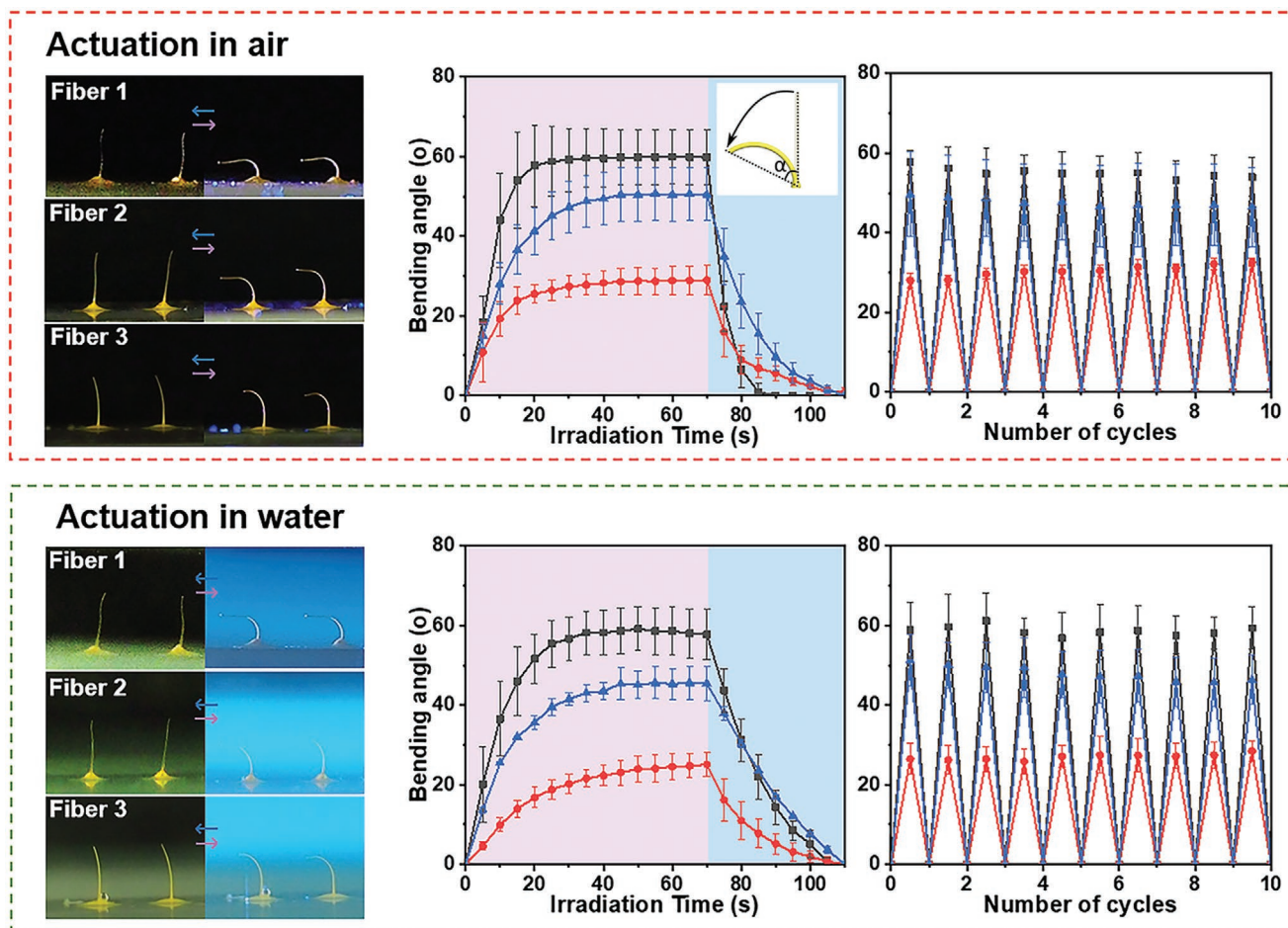
Figure 3. Photomechanical behavior of fibers in air (upper photos) and water (bottom photos). The images of bending and recovery state were taken after illumination with UV light for 70 s and visible light for 40 s. Incident light came from left side. Black, blue, and red lines depict (middle) the bending angle of the fibers (defined in the inset of the middle image) as a function of time and (right) the peak bending angle measured after repeated cycles for fiber 1, fiber 2, and fiber 3, respectively. Fibers from different batches resulted in the errors displayed in the plots.

The fibers were placed in water to further investigate their photo-deformation. Actuation when immersed in water discriminates between photothermal and photochemical actuations. All fibers showed bending–unbending motions upon UV and visible light exposures, respectively. As demonstrated in **Figure 3**, fibers bent only slightly slower in water. The deformation amplitude in air is marginally higher than in water, which hints to a predominantly photochemical actuation in all fibers.

2.3. Light Tracking of Fibers

Light tracking of the fibers was studied under simultaneous illumination with UV and visible light, which resulted in gradients of photoisomerization throughout their diameter. In this study, actuation was achieved through the illumination with UV and visible light sources from opposite directions. The presence of visible light at the opposite side promoted rapid *cis*-to-*trans* back isomerization, overcoming the relatively long *cis* lifetime of azobenzene at ambient temperature.

As presented in **Figure 4**a and Movie S4 in the Supporting Information, fibers continuously tracked UV light 360° azimuthally at room temperature when two light sources were simultaneously rotated with a speed from 2.1 to 9.0° s⁻¹. UV light tracking was further investigated by rotating the fiber without changing the positions of the light sources (Figure 4b and Movie S5, Supporting Information). Again, the bending behavior of the fibers adjusted the bending direction toward the UV light due to the fast transformation between *trans* and *cis* isomer. Such sunflower-like UV-light-tracking movements of fibers can be ascribed to the gradient isomerization and asymmetric shrinkage ratio through the fiber depth.[38,39]

2.4. Light Guiding of Fibers

Additionally, we demonstrated the light guiding behavior in the fibers by integrating them with a red emitting fluorescent dye-doped polymethyl methacrylate (PMMA) plate, which collects light from the environment, e.g. halogen light. The
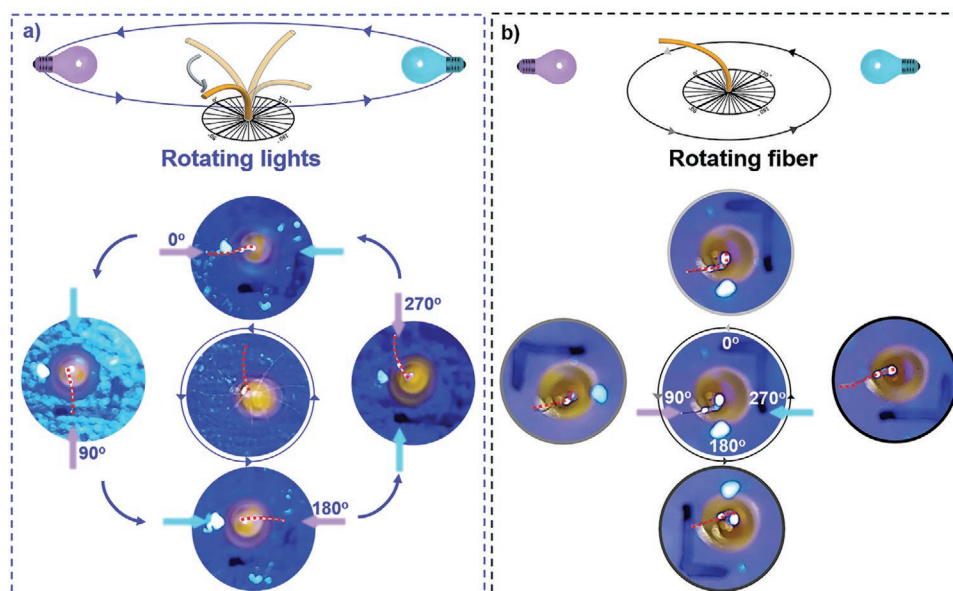
**ADVANCED
SCIENCE NEWS**

www.advancedsciencenews.com

**ADVANCED
OPTICAL
MATERIALS**

www.advopticalmat.de

Figure 4. Self-regulation of fiber 2 at room temperature in air. a) Fixed fibers continuously adjusted their bending direction to follow the rotation of UV and visible light. b) Rotating fibers bent toward the same direction once the position of incident light sources was fixed.

emission light is largely confined in the PMMA plate by total internal reflection.[40–42] The light can be redistributed in space through the vertically positioned fibers which are optically coupled through their matching refractive indices to the polymer plate (see **Figure 5**). Red emission was observed on the tip of the fibers once the dye-doped plate was illuminated with a halogen light. In addition, the direction of emitted light outcoupling was controlled by the bending of the optical fibers, driven by their exposure to UV light. Fibers immediately bent toward the UV light source upon irradiation, and remain bent after the removal of UV light. The extent of bending in fibers was depended on the duration of the UV light illumination.

3. Conclusion

Two types of acrylate-terminated main chain oligomers, with and without azobenzene moieties, were synthesized via thiol-acrylate Michael addition reaction. A drop casting/drawing technique was employed to fabricate a series of fibers array with different LC polymer networks. Altering the location of azobenzene chromophores in the network led to tunable photo-deformation of cilia-like structures in both air and water, indicting the importance of the presence and positioning of the azobenzene in the main chain oligomer. In addition, fibers presented the omnidirectional rotation under simultaneous illumination by UV and visible lights. Finally, the prepared photoresponsive optical fibers
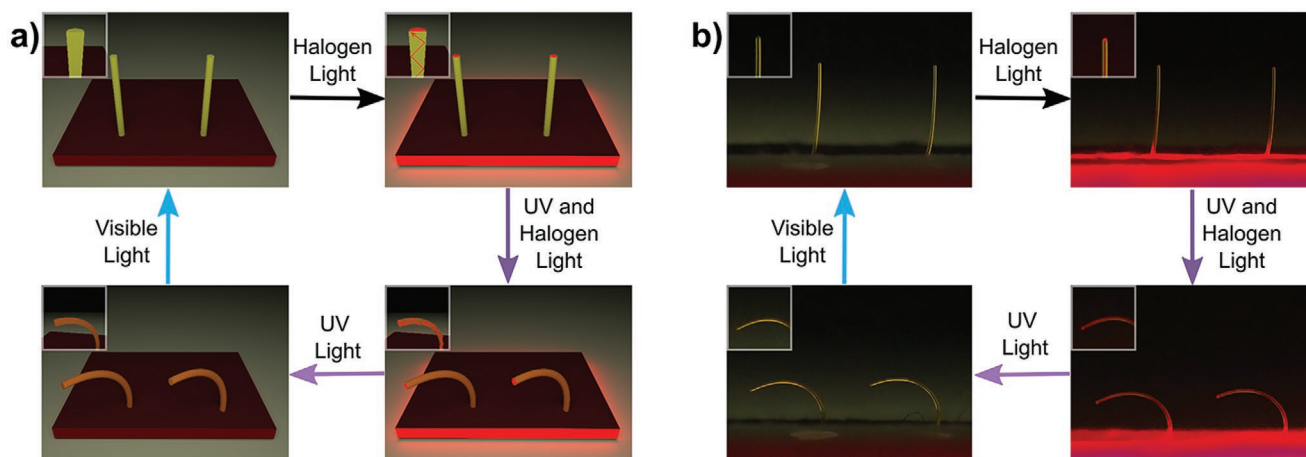

Figure 5. Light tracking behavior of fibers. a) Representative scheme and b) snapshots of fibers illuminated with halogen, UV, or visible light. The inset in the upper left corners corresponds to the schematic a) cross-section of fiber and b) photos of fiber tip, respectively.

exhibited the light guiding properties. We anticipate that photo-induced morphing of the actuator arrays has potential application in advanced optical and aqueous microfluidic devices.

4. Experimental Section

Synthesis of Oligomers: A series of fibers containing 6 wt% azobenzene molecules was fabricated; the molar feed ratios of each oligomer are described in Table S1 in the Supporting Information. First, a mixture of diacrylate mesogens and chain extender 3,6-dioxa-1,8-octanedithiol was dissolved in dichloromethane and continuously stirred. Typically, in the mixture of oligomer 1, diacrylate azobenzene mesogen 3 was added to incorporate azobenzene chromophores into the main chain oligomer. After homogenous mixing, base catalyst triethylamine was slowly added into the reactant. The resultant solution was heated to 38 °C and allowed to react overnight. The crude solution was diluted with dichloromethane (DCM) and then washed with 1 M HCl (twice) and saturated brine (once) to remove residual catalyst. The collected organic phase was then dried by $MgSO_4$. Filtrate was subsequently concentrated by a rotary evaporator, and residual solvent was removed at room temperature via a vacuum oven overnight.

Preparation of Fibers: A mixture of 270 mg oligomer and 5.4 mg photoinitiator Irgacure 819 (2 wt %) was dissolved in 1 mL DCM. 6 wt% 1 and 6 wt% 3 were added to fibers 2 and 3, respectively. A typical 10 µL droplet was drop casted on a 3×3 cm^2 clean glass substrate (sonicated in ethanol and dried by air flow) and placed on a hotplate and heated to 60 °C for 30 min to evaporate the DCM. Subsequently, another glass plate was placed 1.25 cm above the droplet-containing substrate, and the top plate brought into contact with the droplets. Fibers were formed when the two glass plates were pulled apart. The fibers were subsequently photo-crosslinked upon exposure to an EXFO Omnicure S2000 lamp in a nitrogen atmosphere for 1 h. A 405 nm cut-off optical filter was used to limit the *trans*-to-*cis* isomerization of azobenzene during photopolymerization. After photopolymerization, fibers were cut from one side of the glass plate with a scissor to produce desired standing fibers with a length of about 3.5 mm.

Supporting Information

Supporting Information is available from the Wiley Online Library or from the author.

Conflict of Interest

The authors declare no conflict of interest.

Keywords

fiber arrays, light guiding, light tracking, liquid crystals, photoresponsive actuators

[1] M. Pilz da Cunha, S. Ambergen, M. G. Debije, E. F. G. A. Homburg, J. M. J. den Toonder, A. P. H. J. Schenning, *Adv. Sci.* **2020**, *7*, 1902842.

[2] J. Han, W. Jiang, D. Niu, Y. Li, Y. Zhang, B. Lei, H. Liu, Y. Shi, B. Chen, L. Yin, X. Liu, D. Peng, B. Lu, *Adv. Intell. Syst.* **2019**, *1*, 1900109.

[3] C. Ma, W. Lu, X. Yang, J. He, X. Le, L. Wang, J. Zhang, M. J. Serpe, Y. Huang, T. Chen, *Adv. Funct. Mater.* **2018**, *28*, 1704568.

[4] R. C. P. Verpaalen, M. Pilz da Cunha, T. A. P. Engels, M. G. Debije, A. P. H. J. Schenning, *Angew. Chem., Int. Ed.* **2020**, *59*, 4532.

[5] J. Liu, J. Shang, Y. Chen, Y. Tian, Q. Yang, M. Chen, B. Xiong, X. B. Zhang, *J. Mater. Chem. B* **2019**, *7*, 5528.

[6] H. Zhang, H. Zeng, A. Priimagi, O. Ikkala, *Nat. Commun.* **2019**, *10*, 3267.

[7] H. S. Atamian, N. M. Creux, E. A. Brown, A. G. Garner, B. K. Blackman, S. L. Harmer, *Science* **2016**, *353*, 587.

[8] X. Qian, Y. Zhao, Y. Alsaid, X. Wang, M. Hua, T. Galy, H. Gopalakrishna, Y. Yang, J. Cui, N. Liu, M. Marszewski, L. Pilon, H. Jiang, X. He, *Nat. Nanotechnol.* **2019**, *14*, 1048.

[9] A. S. Kuenstler, H. Kim, R. C. Hayward, *Adv. Mater.* **2019**, *31*, 1901216.

[10] L. Liu, M. H. Liu, L. L. Deng, B. P. Lin, H. Yang, *J. Am. Chem. Soc.* **2017**, *139*, 11333.

[11] R. Lan, J. Sun, C. Shen, R. Huang, Z. Zhang, L. Zhang, L. Wang, H. Yang, *Adv. Mater.* **2020**, *32*, 1906319.

[12] H. Tian, Z. Wang, Y. Chen, J. Shao, T. Gao, S. Cai, *ACS Appl. Mater. Interfaces* **2018**, *10*, 8307.

[13] H. Shahsavan, A. Aghakhani, H. Zeng, Y. Guo, Z. S. Davidson, A. Priimagi, M. Sitti, *Proc. Natl. Acad. Sci. USA* **2020**, *117*, 5125.

[14] S. Xie, R. Pennetta, Z. Wang, P. St.J. Russell, *ACS Photonics* **2019**, *6*, 3315.

[15] B. R. Donovan, V. M. Matavulj, S.-K. Ahn, T. Guin, T. J. White, *Adv. Mater.* **2019**, *31*, 1805750.

[16] S. Iamsaard, E. Anger, S. J. Aßhoff, A. Depauw, S. P. Fletcher, N. Katsonis, *Angew. Chem., Int. Ed.* **2016**, *55*, 9908.

[17] A. H. Gelebart, D. Jan Mulder, M. Varga, A. Konya, G. Vantomme, E. W. Meijer, R. L. B. Selinger, D. J. Broer, *Nature* **2017**, *546*, 632.

[18] J. A. Lv, Y. Liu, J. Wei, E. Chen, L. Qin, Y. Yu, *Nature* **2016**, *537*, 179.

[19] X. Pang, J. A. Lv, C. Zhu, L. Qin, Y. Yu, *Adv. Mater.* **2019**, *31*, 1904224.

[20] Y. Yu, M. Nakano, T. Ikeda, *Nature* **2003**, *145*, 425.

[21] H. Kim, J. A. Lee, C. P. Ambulo, H. B. Lee, S. H. Kim, V. V. Naik, C. S. Haines, A. E. Aliev, R. Ovalle-Robles, R. H. Baughman, T. H. Ware, *Adv. Funct. Mater.* **2019**, *29*, 1905063.

[22] T. Ube, T. Ikeda, *Adv. Opt. Mater.* **2019**, *7*, 1900380.

[23] L. Dong, Y. Zhao, *Mater. Chem. Front.* **2018**, *2*, 1932.

[24] M. Mauro, *J. Mater. Chem. B* **2019**, *7*, 4234.

[25] A. H. Gelebart, M. Mc Bride, A. P. H. J. Schenning, C. N. Bowman, D. J. Broer, *Adv. Funct. Mater.* **2016**, *26*, 5322.

[26] T. Yoshino, M. Kondo, J. Mamiya, M. Kinoshita, Y. Yu, T. Ikeda, *Adv. Mater.* **2010**, *22*, 1361.

[27] Z. Cheng, S. Ma, Y. Zhang, S. Huang, Y. Chen, H. Yu, *Macromolecules* **2017**, *50*, 8317.

[28] Y. Liu, W. Wu, J. Wei, Y. Yu, *ACS Appl. Mater. Interfaces* **2017**, *9*, 782.

[29] S. Nocentini, D. Martella, D. S. Wiersma, C. Parmeggiani, *Soft Matter* **2017**, *13*, 8590.

[30] M. O. Saed, A. Gablier, E. M. Terentjev, *Adv. Funct. Mater.* **2020**, *30*, 1906458.

[31] M. Barnes, R. Verduzco, *Soft Matter* **2019**, *15*, 870.

[32] T. H. Ware, Z. P. Perry, C. M. Middleton, S. T. Iacono, T. J. White, *ACS Macro Lett.* **2015**, *4*, 942.

[33] M. O. Saed, C. P. Ambulo, H. Kim, R. De, V. Raval, K. Searles, D. A. Siddiqui, J. M. O. Cue, M. C. Stefan, M. R. Shankar, T. H. Ware, *Adv. Funct. Mater.* **2019**, *29*, 1806412.

[34] T. Guin, M. J. Settle, B. A. Kowalski, A. D. Auguste, R. V. Beblo, G. W. Reich, T. J. White, *Nat. Commun.* **2018**, *9*, 2531.

[35] Y. Xia, X. Zhang, S. Yang, *Angew. Chem., Int. Ed.* **2018**, *57*, 5665.

**ADVANCED
SCIENCE NEWS**

www.advancedsciencenews.com

**ADVANCED
OPTICAL
MATERIALS**

www.advopticalmat.de

[36] J. Küpfer, H. Finkelmann, *Macromol. Chem. Rapid. Commun.* **1991**, *12*, 717.

[37] M. Harada, M. Ochi, M. Tobita, T. Kimura, T. Ishigaki, N. Shimoyama, H. Aoki, *J. Polym. Sci., Part B: Polym. Phys.* **2004**, *42*, 758.

[38] Y. Yao, J. T. Waters, A. V. Shneidman, J. Cui, X. Wang, N. K. Mandsberg, S. Li, A. C. Balazs, J. Aizenberg, *Proc. Natl. Acad. Sci. USA* **2018**, *115*, 12950.

[39] J. T. Waters, S. Li, Y. Yao, M. M. Lerch, M. Aizenberg, J. Aizenberg, A. C. Balazs, *Sci. Adv.* **2020**, *6*, eaay5349.

[40] B. McKenna, R. C. Evans, *Adv. Mater.* **2017**, *29*, 1606491.

[41] J. A. H. P. Sol, G. H. Timmermans, A. J. van Breugel, A. P. H. J. Schenning, M. G. Debije, *Adv. Energy Mater.* **2018**, *8*, 1702922.

[42] M. G. Debije, P. P. C. Verbunt, *Adv. Energy Mater.* **2012**, *2*, 12.